




Cite this: *Food Funct.*, 2018, **9**, 5728

Momordica charantia extracts protect against inhibition of endothelial angiogenesis by advanced glycation endproducts *in vitro*

Ali Aljohi,^{†a} Sabine Matou-Nasri,^{†b} Donghui Liu,^a Nadia Al-Khafaji,^a Mark Slevin^a and Nessar Ahmed  ^{★a}

Diabetes mellitus characterized by hyperglycemia favors formation of advanced glycation endproducts (AGEs) capable of triggering vascular complications by interfering with imbalanced inflammation and angiogenesis to eventually impede wound-healing. *Momordica charantia* (MC, bitter melon) has been shown to prevent AGE formation and to promote angiogenesis in diabetic wounds in animal models. However, the mechanism underlying its effects on angiogenesis is unclear. We investigated the effects of methanolic extracts of MC pulp (MCP), flesh (MCF) and charantin (active component of MC) using an *in vitro* model of angiogenesis. MC extracts or low concentrations of bovine serum albumin-derived AGEs (BSA-AGEs) stimulated proliferation, migration (using wound-healing assay) and tube formation (using Matrigel™-embedded 3D culture) of bovine aortic endothelial cells (BAEC) together with increases in the phosphorylation of extracellular signal-regulated kinase (ERK)1/2, the key angiogenic signaling cytoplasmic protein. Blocking the receptor for AGEs (RAGE) inhibited low BSA-AGE- and MC extract-induced ERK1/2 phosphorylation and tube formation, indicating the crucial role of RAGE in the pro-angiogenic effects of MC extracts. Moreover, inhibitory effects of high BSA-AGE concentration on cell proliferation and migration were reduced by the addition of MC extracts, which reversed the BSA-AGE anti-angiogenic effect on tube formation. Thus, MC extracts exert direct pro-angiogenic signaling mediated via RAGE to overcome the anti-angiogenic effects of high BSA-AGEs, highlighting the biphasic RAGE-dependent mechanisms involved. This study enhances our understanding of the mechanisms underlying the pro-angiogenic effects of MC extracts in improvement of diabetes-impaired wound-healing.

Received 12th February 2018,
Accepted 6th October 2018

DOI: 10.1039/c8fo00297e

rsc.li/food-function

1 Introduction

Diabetes is a chronic metabolic disease characterized by hyperglycemia. It is a major public health problem and now considered as the fourth most common cause of death in most developed countries.¹ Hyperglycemia favors the formation of advanced glycation endproducts (AGEs) as a result of glycation of plasma proteins such as albumin, extracellular matrix proteins such as collagen, lipids or even of nucleic acids like DNA.^{2,3} Increased AGE formation occurs in the kidneys, skin and vascular tissues.^{4–6} High concentration of AGEs affect tissues and cause various adverse cellular events, including increased free radical activity, which can damage cell mem-

branes and promote mutations, alterations in enzymatic activity, cross-linking and impaired degradation of proteins.^{7,8} These biochemical and cellular disturbances lead to the onset of diabetes-related vascular complications.^{9,10}

These vascular complications result from an imbalanced inflammation and from the dysregulation of angiogenesis, defined as the formation of new blood vessels from pre-existent ones. The micro-environment affects the outcome of angiogenic responses in patients with diabetes mellitus. For instance, in the retina, hypervascularization can occur (diabetic retinopathy), whereas in other tissues, including diabetic foot ulcers, significant delays and impaired healing of both acute and chronic wounds are observed.^{11,12} Many studies have described both pro- and anti-angiogenic effects of AGEs, with effects that vary with the concentrations and types of AGEs.^{13,14} These dose-dependent effects mainly involve interaction with the receptor for AGEs (RAGE), a 45 kDa transmembrane multi-ligand receptor belonging to the immunoglobulin superfamily, with the ability to transduce a bell-shaped curve cell response indicating a bivalent bridging mechanism.¹⁵

^aSchool of Healthcare Science, Manchester Metropolitan University, Manchester M1 5GD, UK. E-mail: N.Ahmed@mmu.ac.uk; Fax: +44(0) 161 247 6831;

Tel: +44(0) 161 247 1163

^bKing Abdullah International Medical Research Center, Medical Genomics Research Department, National Guard Health Affairs, Riyadh 11426, Saudi Arabia

[†]These authors equally contributed to the work.



This bivalent mechanism is explained on the one hand by the induction of the cell response after dimerization/oligomerization of the receptor facilitated by a low ligand concentration and, on the other hand; by the loss/inhibition of the cell response due to the impediment of the receptor oligomerization at high ligand concentrations.¹⁵ Ligation of RAGE leads to activation of phosphorylated extracellular signal-regulated kinase (p-ERK)-1/2, the key angiogenic signaling protein.^{16–18}

Momordica Charantia Linn (MC) is a member of the *Cucurbitaceae* family and is also known as bitter melon, bitter gourd, balsam pear in English or Karela in Hindi. Its fruit is eaten in many Asian countries including Pakistan, India, Nepal, China, and in tropical Africa.¹⁹ MC primarily consists of glycosides, proteins, saponins, reducing sugars, sterols, fatty acids and volatile constituents,²⁰ and contains biologically active chemicals such as charantins (mixtures of steroidal saponins also called momocharins), insulin-like peptides (called 'polypeptide-P'), and alkaloids with hypoglycemic effects (e.g. momordicin presents in seed) and ascorbigens, bound forms of ascorbic acid.^{20,21} Charantin is a non-nitrogenous neutral mixture of steroidal saponins, composed of sitosterol glucoside and stigmasteryl glucoside.²⁰ The fruit pulp, the leaf juice and the seeds of MC have been consumed as dietary supplements and used in ethno-medicine for centuries^{22–24} for their hypolipidemic, antioxidant,²⁵ contraceptive,²⁶ and anti-bacterial properties.²⁷ The products of this plant have been shown to have anti-inflammatory,²⁸ anticancer,²⁹ anti-ulcerogenic activities³⁰ and wound-healing³¹ activities.

Recently, many studies have reported beneficial effects of MC extracts on wound-healing.^{32–34} Using normal rats and rats with diabetes induced by streptozotocin, it has been shown that the administration of dried MC extracts improved and accelerated the process of healing in wounded skin.³² This effect was accompanied by a significant increase in the protein content of the skin in the MC extract-treated diabetic group compared with the untreated diabetic group, suggesting that MC extracts may stimulate cell proliferation through an unknown mechanism.³² An extract of the leaves of MC (in benzene and 95% ethanol) significantly increased the rates of wound closure and epithelialization compared with untreated animals.³³ Topical application of an olive oil extract of MC to wounded rabbit skin or the topical application of aqueous extract of seed and outer layer of MC onto full-thickness skin wounds in albino rats also promoted wound-healing.^{31,34} Recently using a wound chamber model in rats, local application of MC extracts has been reported to promote granulation tissue growth and angiogenesis in the diabetic wound.³⁵ However, the molecular mechanisms involved in the pro-angiogenic effects of MC extracts and charantin have not yet been described.

Here, we demonstrate that MC extracts and charantin promote angiogenesis *in vitro* using endothelial cell proliferation, migration, tube formation and phosphorylation of ERK1/2 through RAGE. We also showed that these MC extracts and charantin reduced the anti-angiogenic effects of high con-

centration of AGEs using cell proliferation and wound-healing assays, while it was reversed using tube formation assay.

This investigation could help us improve our understanding of the wound-healing capacity of these substances in diabetic patients in order to enhance their beneficial effects for the prevention of diabetic vascular complications.

2 Materials and methods

2.1 Preparation of *Momordica charantia* (MC) extracts and charantin

Extracts of the outer layer (the flesh, MCF) and of the seed part (the pulp, MCP) of MC were prepared according to a modification of a previously described method.²² Briefly, the MCF and MCP (130 mg) were extracted using methanol at a 1:10 ratio. Homogenization was performed in a blender using 1-minute bursts at the highest speed for 12 minutes. The homogenized extract was filtered through cheesecloth. A rotary evaporator was used to remove most of the methanol, and any remaining methanol evaporated using a water bath at 100 °C. Charantin was provided by Xi'an Day Natural Technology (Xi'an City, China). Bacterial endotoxins were removed from the extracts and charantin using detoxi-gel endotoxin-removing gel columns (Thermo Scientific, Rockford, USA) and the endotoxins quantified were below the detection limit (<0.125 EU mL⁻¹) as measured by the E-toxate kit based on the *Limulus Amebocyte* lysate assay.

2.2 Preparation of bovine serum albumin-derived advanced glycation endproducts (BSA-AGEs)

BSA-AGEs were prepared and estimated as described previously.³⁶ Briefly, bovine serum albumin (BSA) fraction V (10 mg mL⁻¹) was incubated at 37 °C for different time periods with 0.1 M methylglyoxal in 0.1 M sodium phosphate buffer (pH 7.4) containing 3 mM sodium azide. Controls were incubated under the same conditions without addition of sugars or extracts. All incubations were carried out in triplicate. After incubation, un-reacted sugars were removed by exhaustive dialysis against distilled water for 2 days at 4 °C. BSA-AGE formation was assessed using a fluorescence spectrophotometer (Luminescence spectrometer model LS 30, PerkinElmer LAS Ltd, Buckinghamshire, UK) with excitation at 350 nm and emission at 420 nm. The endotoxin content of all protein solutions were below the detection limit (<0.125 EU mL⁻¹). Protein concentrations were determined using a Bradford-based assay with BSA as a standard.

2.3 Culture of bovine aortic endothelial cells

Tissue for primary cultures of bovine aortic endothelial cells (BAEC) was obtained from the Manchester slaughterhouse and cells isolated and characterized as described previously.³⁷ The cells were cultured in complete medium composed of 15% fetal bovine serum (FBS) in Dulbecco's modified Eagle medium (DMEM) supplemented with 2 mM L-glutamine, 100 IU mL⁻¹ penicillin and 100 µg mL⁻¹ streptomycin and seeded



in tissue culture T-25 flasks coated with 0.1% gelatin. The culture flasks were maintained at 37 °C in a humidified atmosphere of 95% air and 5% CO₂. Every 2–3 days, on reaching confluence, the cells were passaged using enzymatic digestion with 0.05% trypsin/0.02% ethylene-diamine-tetra-acetic acid (EDTA) and split at a ratio of 1 : 2. Throughout the study, the cells used were between passages 4 and 12.

2.4 Cell proliferation assay

BAEC (2.5×10^4 mL⁻¹) in 1 mL of complete medium per well were seeded into 24-well plates (Nunc™, Fisher Scientific, Loughborough, UK). The cells were incubated for 4 hours, allowing them to adhere to the bottom of the wells. The complete medium was discarded, and the cells washed twice with sterile phosphate-buffered saline (PBS). Fresh media supplemented with 2.5% FBS, defined as serum-poor medium (SPM), was added to each well. Extracts and charantin (10, 50 or 75 µg mL⁻¹) were added to the wells and incubated for 72 hours. Untreated cells cultured in SPM and cells treated with the pro-angiogenic growth factor FGF-2 (25 ng mL⁻¹) were used as negative and positive controls, respectively. In separate experiments, BSA-AGEs (250 µg mL⁻¹) were added to the wells with or without extracts and charantin (10 µg mL⁻¹). After incubation for 72 hours, the cells were washed three times with PBS and detached *via* incubation for 5 minutes in 250 µL of 0.05% trypsin/0.02% EDTA. Each cell suspension was diluted in 10 mL of isotonic solution prior to counting using a Beckman-Coulter counter (Buckinghamshire, UK). Each experiment was carried out in triplicate and repeated three times independently. Cell viability was assessed using trypan blue exclusion method, which stains dead cells while viable cells exclude the dye. The percentage cell viability was obtained using an automated cell counter TC10 (Bio-Rad Laboratories) and determined according to the following formula: % viability = (viable unstained cells)/(viable unstained cells + dead stained cells) × 100.

2.5 Cell migration – wound healing assay

A sterile Thermanox® plastic coverslips (Nunc™) was placed into each well of a 24-well plate. BAEC (6×10^4 mL⁻¹) in 1 mL of complete medium were seeded onto each coverslip. After 48 hours of incubation (pre-confluence), the complete medium was replaced with SPM to reduce cell growth, and the cells incubated for a further 24 hours. The cell monolayer attached to the coverslip was washed twice with sterile PBS and then wounded on each side of the central area with a sterile razor blade to produce straight-edged cuts. The wounded cell monolayer was washed three times with sterile PBS to remove cellular debris and dislodged cells, and then placed in a new 24-well plate containing fresh SPM. Various concentrations of extracts and charantin (10, 50 or 75 µg mL⁻¹) were added to the wells and incubated for 24 hours. Untreated cells in SPM and cells treated with FGF-2 (25 ng mL⁻¹) were used as negative and positive controls, respectively. In separate experiments, BSA-AGEs (250 µg mL⁻¹) were added to the wells with or without extracts or charantin (10 µg mL⁻¹). After incubating for 24 hours, the coverslips were rinsed three times with PBS, fixed in 100% ethanol for 5 minutes, and allowed to air-dry. The cells were stained with methylene blue for 5 minutes and excess stain removed with distilled water. Photomicrographs (40× magnification) were taken of 5 randomly selected areas with straight wound edges on each coverslip using a Zeiss phase-contrast microscopy equipped with a digital camera. Migration of cells in each field of view was quantified by counting the migrated cells and by measuring their distance from the wound edge using Image J software (<http://rsbweb.nih.gov/ij/indix.html>). Each experiment was carried out in triplicate, and repeated three times independently.

BAEC (1×10^6 per 32 µL) were mixed with various concentrations of extracts and charantin (10, 50 or 75 µg mL⁻¹) and then in equal volume with growth factor-reduced Matrigel™ (Becton Dickinson, Oxford, UK). BSA-AGEs (250 µg mL⁻¹) were also tested with or without extracts or charantin (10 µg mL⁻¹). Each mixture was deposited equally under a spot shape into two wells of a 48-well plate (Nunc™) per experimental condition. Untreated cells in SPM and cells treated with FGF-2 (25 ng mL⁻¹) were used as negative and positive controls, respectively. Each condition was tested in duplicate. After polymerization of the gel for 1 hour at 37 °C, each spot containing the cells embedded in Matrigel™ was bathed in 500 µL of complete medium. After incubation for 24 hours, some cells had migrated and aligned surrounding an enclosed area. Cells were fixed with 4% paraformaldehyde for 15 minutes and the enclosed areas, used for quantification of tubulogenesis,³⁸ were counted in 5 random fields using phase-contrast microscopy (40× magnification).

2.6 Matrigel™ tube formation assay

BAEC (3×10^5 mL⁻¹) in 1 mL of complete medium per well were seeded into 24-well plates. After incubation for 24 hours (pre-confluence), the medium was discarded, and cells washed three times with PBS. Fresh SPM was added to each well for an additional 24 hours of incubation. Various concentrations of extracts and charantin (10, 50 or 75 µg mL⁻¹) were added to the wells and incubated for 10 minutes. BSA-AGEs (250 µg mL⁻¹) were also tested with or without extracts and charantin (10 µg mL⁻¹). Untreated cells in SPM and cells treated with FGF-2 (25 ng mL⁻¹) were used as negative and positive controls, respectively. Each condition was assayed in triplicate. Immediately after incubation, medium was discarded, and the cells were rinsed twice with cold PBS. After rinsing, intracellular proteins were extracted by lysing the cells with 100 µL per well of ice-cold radioimmunoprecipitation (RIPA) buffer (pH 7.5) containing 25 mM Tris-HCl, 150 mM NaCl, 0.5% sodium deoxycholate, 0.5% SDS, 1 mM EDTA, 1 mM sodium orthovanadate, 1 mM phenylmethylsulfonyl fluoride (PMSF), 1% Triton X-100 and 1 µM leupeptin. Cell lysates were centrifuged for 30 minutes at 20 000g at 4 °C to remove any debris. The protein concentration in each sample was determined using a

2.7 Western blot analysis

BAEC (3×10^5 mL⁻¹) in 1 mL of complete medium per well were seeded into 24-well plates. After incubation for 24 hours (pre-confluence), the medium was discarded, and cells washed three times with PBS. Fresh SPM was added to each well for an additional 24 hours of incubation. Various concentrations of extracts and charantin (10, 50 or 75 µg mL⁻¹) were added to the wells and incubated for 10 minutes. BSA-AGEs (250 µg mL⁻¹) were also tested with or without extracts and charantin (10 µg mL⁻¹). Untreated cells in SPM and cells treated with FGF-2 (25 ng mL⁻¹) were used as negative and positive controls, respectively. Each condition was assayed in triplicate. Immediately after incubation, medium was discarded, and the cells were rinsed twice with cold PBS. After rinsing, intracellular proteins were extracted by lysing the cells with 100 µL per well of ice-cold radioimmunoprecipitation (RIPA) buffer (pH 7.5) containing 25 mM Tris-HCl, 150 mM NaCl, 0.5% sodium deoxycholate, 0.5% SDS, 1 mM EDTA, 1 mM sodium orthovanadate, 1 mM phenylmethylsulfonyl fluoride (PMSF), 1% Triton X-100 and 1 µM leupeptin. Cell lysates were centrifuged for 30 minutes at 20 000g at 4 °C to remove any debris. The protein concentration in each sample was determined using a



Bio-Rad protein assay. The volume of each sample containing 20 μg of protein was combined with an equal volume of 2 \times sample buffer in Eppendorf tubes, mixed, and then placed in boiling water for 15 minutes. The samples were separated along with pre-stained molecular weight markers using sodium dodecyl sulfate – polyacrylamide gel electrophoresis (SDS-PAGE) on 12% acrylamide gels. The proteins were transferred to nitrocellulose membranes (1 hour) and the membranes were blocked for 1 hour at room temperature in Tris-buffered saline (TBS)-Tween (pH 7.4) containing 1% BSA. The membranes were stained overnight at 4 $^{\circ}\text{C}$ on a rotating platform with the following primary antibodies diluted in a blocking buffer: a mouse monoclonal antibody to phospho-extracellular signal-regulated kinase (p-ERK1/2, Tyr204 of ERK1, 1:1000 dilution) and a rabbit polyclonal antibody to total ERK1/2 (t-ERK1/2, 1:1000 dilution), both purchased from Santa Cruz Biotechnology (Heidelberg, Germany). After washing five times for 10 minutes in TBS-Tween at room temperature, the membranes were stained with either horseradish peroxidase rabbit anti-mouse or goat anti-rabbit secondary antibodies diluted in TBS-Tween containing 5% non-fat milk (1:1000 dilution) for 1 hour at room temperature with continuous mixing. After 5 additional washes in TBS-Tween, proteins were visualized using the ECL chemiluminescent detection reagent (Amersham Biosciences, Buckinghamshire, UK) and analyzed using GeneSnap software with Gene tool image analyzer (Syngene, Cambridge, UK).

2.8 RAGE neutralization

To investigate whether the extracts and charantin act through RAGE to induce angiogenic signaling *via* ERK1/2 phosphorylation and tube formation, the cells were treated with anti-RAGE antibody to neutralize the RAGE receptors. Briefly, BAEC in complete medium were seeded in wells of a 24-well plate according to the western blotting protocol above. The medium was replaced with SPM, and then 20 $\mu\text{g mL}^{-1}$ of mouse monoclonal anti-RAGE [E-1] antibody (Santa Cruz Biotechnology) or 20 $\mu\text{g mL}^{-1}$ of isotype control (IgG₁). After incubation for 2 hours, cells were treated with extracts or BSA-AGEs (10 $\mu\text{g mL}^{-1}$) for 10 minutes at 37 $^{\circ}\text{C}$ followed by protein extraction for p-ERK1/2 protein detection using western blotting. The cells were also subjected to the tube formation assay described above with the difference that the cells were initially scraped to maintain the intact RAGE structure. Anti-RAGE antibody or IgG₁ was added to the cold Eppendorf tube containing cells for 1 hour on ice before the addition of extracts or charantin (10 $\mu\text{g mL}^{-1}$) and growth factor-reduced Matrigel™. Each condition was tested in triplicate and each experiment repeated three times.

2.9 Statistical analysis

Statistical analysis was performed using Microsoft Office Excel 2007 and results expressed as mean \pm SD. Statistical significance was analyzed using Student's *t*-test and *p* values ≤ 0.05 were considered significantly different.

3 Results

3.1 *Momordica charantia* extracts are pro-angiogenic *in vitro*

The effects of 72-hour incubation with the MCP, MCF extracts and charantin at concentrations between 10 and 75 $\mu\text{g mL}^{-1}$ on BAEC are shown in Fig. 1A. Compared to the untreated cells considered as negative control, pro-angiogenic growth factor FGF-2 was used as a positive control to confirm the ability of the cells to respond: it induced a significant increase in cell number (67%, $p = 0.0252$, Fig. 1A). The exposure of BAEC to increasing concentrations of MC extracts or charantin significantly enhanced cell proliferation in a dose-dependent manner, with a peak of stimulation found at an intermediate concentration (50 $\mu\text{g mL}^{-1}$) of the extracts (Fig. 1A). Specifically, 10, 50 and 75 $\mu\text{g mL}^{-1}$ of MCP increased BAEC proliferation by 76% ($p = 0.024$), 125% ($p = 0.0259$) and 83% ($p = 0.0281$), respectively, relative to the negative control (Fig. 1A). Similarly, the same concentrations of MCF increased cell growth by 69% (10 $\mu\text{g mL}^{-1}$, $p = 0.0251$), 117% (50 $\mu\text{g mL}^{-1}$, $p = 0.0277$) and 81% (75 $\mu\text{g mL}^{-1}$, $p = 0.0261$), compared to negative control. Charantin at the same concentrations increased BAEC proliferation by 43% (10 $\mu\text{g mL}^{-1}$, $p = 0.0254$), 103% (50 $\mu\text{g mL}^{-1}$, $p = 0.0273$) and 50% (75 $\mu\text{g mL}^{-1}$, $p = 0.0197$) when compared with the negative control (Fig. 1A).

Because cell migration is an essential step in angiogenesis, it was also important to evaluate the effects of MCP, MCF and charantin on BAEC migration using an *in vitro* injury model such as wound-healing assay (Fig. 1B). Compared with the untreated cells, the negative control (Fig. 1Bi); FGF-2 (25 ng mL^{-1} , Fig. 1Bii), used as a positive control, significantly increased the cell migration distance by 26.5% ($p = 0.0282$) and the number of migrated cells by 47% ($p = 0.0284$, Fig. 1B). At 10 $\mu\text{g mL}^{-1}$, MCP significantly increased BAEC migration to a level similar to FGF-2: the migration distance was increased by 27% ($p = 0.0284$) and the number of migrated cells was increased by 43% ($p = 0.0284$) relative to the negative control (Fig. 1Biii and Bvi). At 50 $\mu\text{g mL}^{-1}$, MCP significantly increased the distance of migration by approximately 15% ($p < 0.05$), and the cell number increased by 33% ($p = 0.0288$). However, 75 $\mu\text{g mL}^{-1}$ MCP did not affect either the cell migration distance or number (Fig. 1Bvi). Furthermore, MCF (Fig. 1Biv and Bvii) and charantin (Fig. 1Bv and Bviii) enhanced the distance of migration by 15% at all concentrations used. However, the highest response to increase the number of migrated cells was found at 50 $\mu\text{g mL}^{-1}$ of MCF (45%, $p = 0.0281$) or charantin (40%, $p = 0.0286$) as compared with the negative control (Fig. 1B).

To evaluate the effects of the MC extracts on the last step of angiogenesis, endothelial cell differentiation was assessed by the tube formation assay using a 3-D Matrigel™ culture. Within 24 hours of incubation, the activated endothelial cells migrated, aligned to form tubes organized in a capillary-like network (Fig. 1C). Representative photomicrographs of the tube formation in the untreated condition (Fig. 1Ci), or after treatment with either FGF-2 (Fig. 1Cii), or 10 $\mu\text{g mL}^{-1}$ of MCP



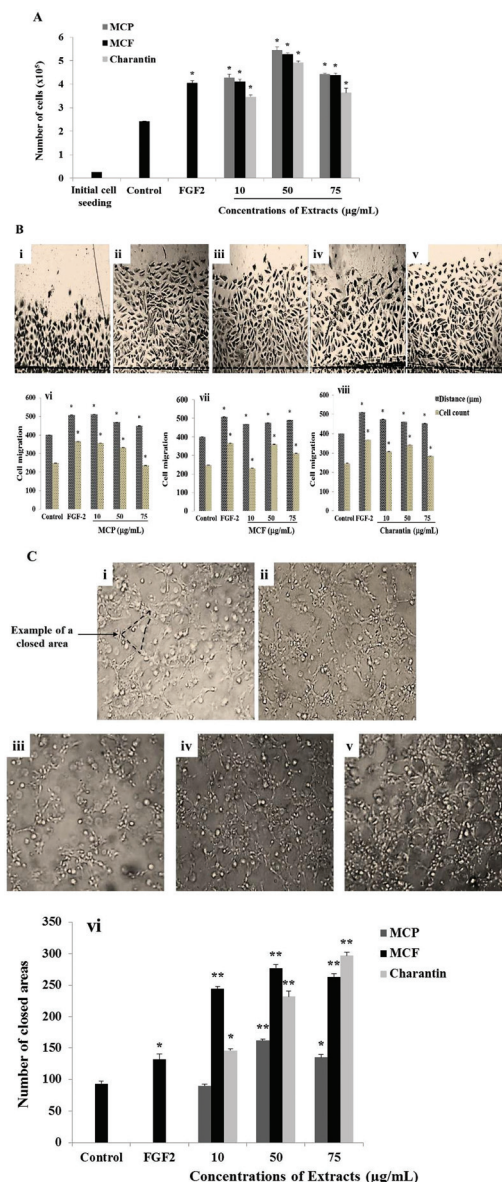


Fig. 1 Effects of *Momordica charantia* extracts on proliferation, migration and tube formation of BAEC. (A) Untreated BAEC (control) or those treated either with 25 ng mL⁻¹ FGF-2, or various concentrations of MCP, MCF or charantin for 72 hours of incubation. The bar graph shows the stimulatory effects of MCP, MCF and charantin. The data are presented as the mean \pm SD ($n = 3$). (B) Representative photomicrographs (40 \times magnification) show the BAEC measured from the wound edge (indicated by dashed lines) after incubation for 24 hours for untreated cells (i), or those treated with FGF-2 (ii) or 10 μ g mL⁻¹ of MCP (iii), MCF (iv) or charantin (v). The bar graphs show the number of migrated cells (dark bars) and the distance of migration (clear bars) of the BAEC under these conditions including the three concentrations of MCP (vi), MCF (vii) and charantin (viii). The data are presented as the mean \pm SD ($n = 3$). (C) Representative photomicrographs (40 \times magnification) showing the BAEC tube formation after a 24-hour incubation in untreated cells (i), and those treated with FGF-2 (ii) or 10 μ g mL⁻¹ of MCP (iii), MCF (iv) or charantin (v). The enclosed areas (an example as indicated by the arrow) were counted as a parameter for quantification of tubulogenesis. The bar graphs (vi) show the effects of MCP, MCF extracts and charantin respectively on tube formation. The data are presented as the mean \pm SD ($n = 3$). (*) and (**) indicate statistically significant differences ($p < 0.05$ and $p < 0.01$ respectively) from the control.

(Fig. 1Ciii), MCF (Fig. 1Civ) and charantin (Fig. 1Cv) are shown. Treatment with the positive control, FGF-2, stimulated the cells to form a capillary-like network (Fig. 1Cii). A significant increase of 42% ($p = 0.048$) in the network density was observed in the FGF-2-treated cells compared with the negative untreated control cells, which formed a few tube-like structures (Fig. 1C). Although no effect was noticed at the lowest concentration of MCP, in the presence of 50 and 75 μ g mL⁻¹ MCP, the tube formation significantly increased by 74% ($p = 0.0093$) and 41% ($p = 0.046$), respectively, compared with the negative control (Fig. 1Cvi). All concentrations of MCF significantly enhanced tube formation relative to the negative control: 162% ($p = 0.0082$) at 10 μ g mL⁻¹, 197% ($p = 0.0078$) at 50 μ g mL⁻¹ and 182% ($p = 0.0079$) at 75 μ g mL⁻¹ (Fig. 1Cvi). Charantin also significantly enhanced the endothelial tube formation in a concentration-dependent manner (Fig. 1Cvi). Specifically, 10, 50 and 75 μ g mL⁻¹ of charantin significantly increased the number of enclosed areas by 57% ($p = 0.049$), by 149% ($p = 0.0076$) and 219% ($p = 0.0079$), respectively, compared with the negative control (Fig. 1Cvi).

3.2 *Momordica charantia* extracts increase the phosphorylation of angiogenic signaling protein ERK1/2

Because the activation of ERK1/2 is considered as the key step of angiogenesis,¹⁷ phospho-ERK1/2 (p-ERK1/2) expression levels in presence of the MC extracts and charantin were examined. To optimize the incubation time corresponding to the maximal cell signaling induced by MC extracts at the concentrations showing similar effects than FGF-2 (positive control), western blotting was used to determine the levels of p-ERK1/2 expression in BAEC treated with 10 μ g mL⁻¹ MCP (MC extract with strongest pro-mitogenic effect) for 10 minutes and 1, 3 or 6 hours of incubation. After 10 minutes of incubation of the cells with MCP, the phosphorylation of ERK1/2 was significantly increased (5.0-fold, $p < 0.01$, Fig. 2) compared with the basal level of p-ERK1/2 expressed in untreated (negative) control cells. This effect was similar to that of FGF-2 (Fig. 2). The level of p-ERK1 slightly decreased at the 1-hour time point, and had nearly disappeared after 6 hours (Fig. 2).

Fig. 3 shows a representative western blot using BAEC lysate proteins after a 10-minute treatment of the cells with different concentrations (10, 50 or 75 μ g mL⁻¹) of the MC extracts or charantin or the positive control, FGF-2. As expected, treatment with FGF-2 significantly induced the p-ERK1/2: a 5.5-fold ($p < 0.001$) increase in p-ERK2 and a 1.9-fold ($p < 0.01$) increase in p-ERK1 were observed compared with the basal levels of p-ERK1/2 in untreated control cells (Fig. 3). Treatment of the cells with MCP (Fig. 3A), MCF (Fig. 3B) and charantin (Fig. 3C) significantly ($p < 0.01$) increased the levels of p-ERK1/2 in a dose-dependent manner, with the highest response found at 50 μ g mL⁻¹ of MCP (4.7-fold increase of p-ERK2 expression, 1.8-fold increase of p-ERK1 expression; Fig. 3A), MCF (4.5-fold increase p-ERK2, 1.8-fold p-ERK1 expression; Fig. 3B) or charantin (3.79-fold of p-ERK2 expression, 1.23-fold p-ERK1 expression; Fig. 3C), compared with the negative control.



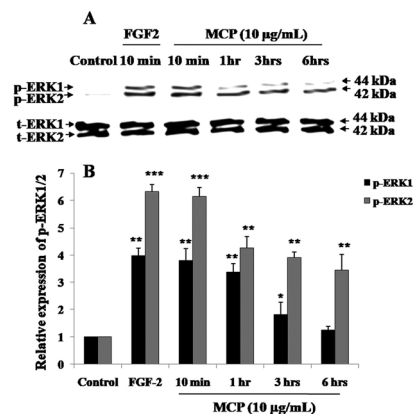


Fig. 2 Time course of angiogenic signaling p-ERK1/2 levels in BAEC treated with $10 \mu\text{g mL}^{-1}$ of the MCP extract. (A) Representative western blot analysis showing the effect of FGF-2 (positive control, 10 minutes incubation) and of $10 \mu\text{g mL}^{-1}$ MCP extract on the p-ERK1/2 levels in BAEC after 10 minutes, 1 hour, 3 hours and 6 hours of incubation as compared with the untreated cells (control). Total ERK1/2 expression was used as a loading control. (B) Bar graph showing the densitometric quantification of the bands expressed as values relative to total-ERK1/2 levels and calculated as the ratio to the levels in the control cultures. The results are presented as the mean \pm SD ($n = 3$). (*), (**) and (***) signify statistically significant differences ($p < 0.05$, $p < 0.01$ and $p < 0.001$, respectively) from the control.

3.3 Biphasic dose-dependent effects of BSA-AGEs on p-ERK1/2 levels

To determine the effects of different concentrations of BSA-AGEs on phosphorylation of key angiogenic signaling molecules ERK1/2, BAEC were stimulated with BSA-AGEs (25 , 50 , 100 or $250 \mu\text{g mL}^{-1}$) for 10 minutes. At these various concentrations, BSA-AGEs modulated ERK1/2 phosphorylation in a dose-dependent manner and showed biphasic effects. Indeed, at 50 – $100 \mu\text{g mL}^{-1}$ of BSA-AGEs, a significant ($p < 0.01$) increase in the phosphorylation of ERK1/2 was observed (around 4.0-fold increase of p-ERK1, around 4.5-fold increase of p-ERK2), while $250 \mu\text{g mL}^{-1}$ BSA-AGEs inhibited ERK1/2 phosphorylation, compared with the level of p-ERK1/2 in untreated control cells (Fig. 4). At the lowest concentration ($25 \mu\text{g mL}^{-1}$), BSA-AGEs did not change ERK1/2 phosphorylation level as compared with the level of p-ERK1/2 detected in untreated control cells (Fig. 4).

3.4 *Momordica charantia* extracts reduce anti-angiogenic effects of BSA-AGEs

MC extracts have beneficial effects on delayed wound-healing observed in diabetic patients *in vivo*. To investigate the molecular mechanisms involved, the effects of MC extracts and charantin were tested using the *in vitro* angiogenesis assays. The high concentration of BSA-AGEs ($250 \mu\text{g mL}^{-1}$) inhibited BAEC proliferation by 70% relative to the negative control, the untreated cell population (Fig. 5A), but native BSA had no effect (data not shown). The addition of $10 \mu\text{g mL}^{-1}$ of the MCP significantly reduced the inhibitory effect of BSA-AGEs

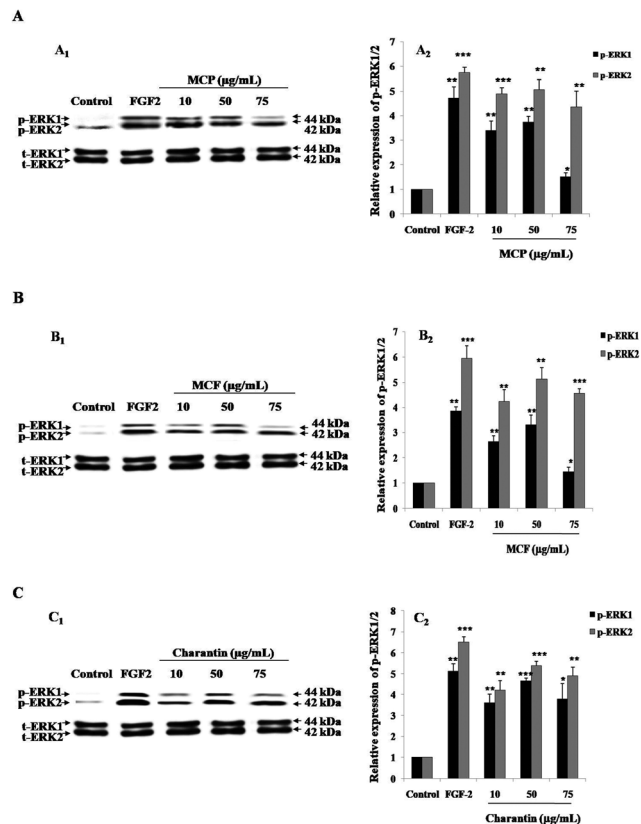


Fig. 3 *Momordica charantia* extracts increase p-ERK1/2 levels in cultured BAEC. Representative western blots showing the levels of p-ERK1/2 induced by 10 – $75 \mu\text{g mL}^{-1}$ of MCP (A₁) or MCF (B₁) extracts and charantin (C₁) after a 10-minute incubation. The bar graphs show the p-ERK1/2 expression levels induced by MCP (A₂), MCF (B₂) extracts and charantin (C₂). The data show the densitometric quantification of the bands expressed as values relative to total-ERK1/2 levels and calculated as the ratio to the levels in the control cultures. The results are presented as the mean \pm SD ($n = 3$). (*), (**) and (***) signify statistically significant differences ($p < 0.05$, $p < 0.01$ and $p < 0.001$, respectively) from the control.

on the proliferation of BAEC by 1.9-fold ($p = 0.0068$), compared with the negative control. Similarly, the MCF extract or charantin reduced the inhibitory effect of BSA-AGEs by 1.7-fold ($p = 0.009$) (Fig. 5A). There were no effects of any of the extracts, BSA-AGEs or native BSA on the cell viability (data not shown). To determine whether the MC extracts altered the effects of a high concentration of BSA-AGEs ($250 \mu\text{g mL}^{-1}$) on the migration of BAEC (Fig. 5B), representative photomicrographs of the migration of untreated cells (Fig. 5Bi) or cells treated with FGF-2 (Fig. 5Bii), BSA-AGEs (Fig. 5Biii) or BSA-AGEs combined with MCP (Fig. 5Biv), MCF (Fig. 5Bv) or charantin (Fig. 5Bvi) were evaluated. Treatment of the cells with the high concentration of BSA-AGEs decreased the cell migration distance by 50% ($p = 0.028$) and the number of migrated cells by 40% ($p = 0.026$), compared to the negative control. Native BSA at $250 \mu\text{g mL}^{-1}$ did not affect cell migration (data not shown). The addition of MCP and MCF extracts reduced the inhibitory effect of the BSA-AGEs on BAEC migration distance by approxi-



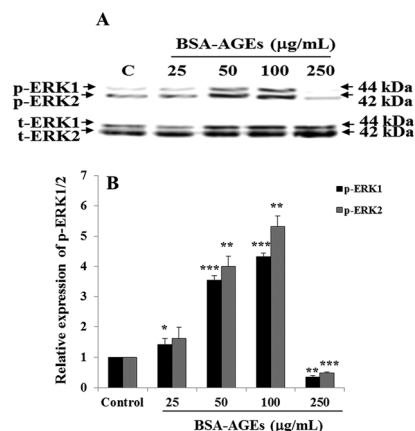


Fig. 4 Biphasic effects of BSA-AGEs on p-ERK1/2 levels in a dose-dependent manner. (A) Representative western blot analysis showing the levels of p-ERK1/2 after a 10-minute incubation with a range of concentrations of BSA-AGEs. (B) The bar graph shows the densitometric quantification of the bands expressed as values relative to total-ERK1/2 levels and calculated as the ratio to the levels in the control cultures. The results are presented as the mean \pm SD ($n = 3$). (*), (**) and (***) signify statistically significant differences ($p < 0.05$, $p < 0.01$ and $p < 0.001$, respectively) from the control.

mately 1.5-fold ($p < 0.05$) and the number of migrated cells by approximately 1.6-fold ($p < 0.05$), compared to the cells treated with BSA-AGEs (Fig. 5Bvii). Charantin also reduced the inhibitory effect of BSA-AGEs on the migration distance by 1.28-fold ($p = 0.035$) and the number of migrated cells by approximately 1.29-fold ($p = 0.025$) (Fig. 5Bvii).

Representative photomicrographs of the tube formation in cells treated with $250 \mu\text{g mL}^{-1}$ BSA-AGEs (Fig. 5Ci) or BSA-AGEs combined with $10 \mu\text{g mL}^{-1}$ MCP (Fig. 5Cii), MCP (Fig. 5Ciii) or charantin (Fig. 5Civ) are shown. The high concentration of BSA-AGEs significantly decreased the tube formation by 0.67-fold ($p = 0.014$; Fig. 5Cv) as compared with the control, while native BSA had no effect (data not shown). The addition of the MC extracts (MCP and MCF) to the high concentration of BSA-AGEs not only suppressed the inhibitory effect of BSA-AGEs on BAEC tube formation but actually significantly increased the tube formation by 2.7-fold ($p < 0.01$), compared to the BSA-AGEs-treated cells (Fig. 5Cv). The addition of charantin to the high concentration of BSA-AGEs also reduced the inhibitory effect of the BSA-AGEs on BAEC tube formation and slightly increased the tubulogenesis process by 1.5-fold ($p = 0.013$) as compared to the BSA-AGEs treated cells (Fig. 5Cv).

3.5 *Momordica charantia* extracts exert endothelial angiogenic functions through RAGE

We next wondered whether MC extracts and charantin acted through RAGE as AGEs do and thus, explain how MC extracts interfere in the angiogenic effects of AGEs. This hypothesis was verified based on the induced phosphorylation of angiogenic signaling protein ERK1/2 and on tube formation. The receptor was neutralized using an anti-RAGE antibody at a con-

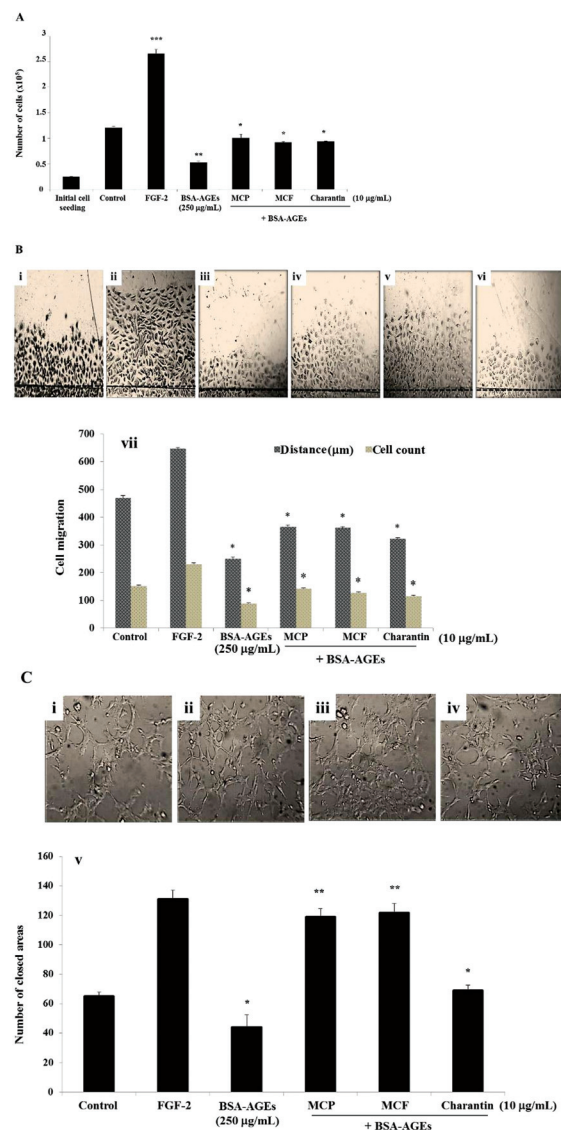


Fig. 5 Effects of *Momordica charantia* extracts on proliferation, migration and tube formation of BAEC exposed to high concentrations of BSA-AGEs. (A) Untreated BAEC (control) or those treated for a 72-hour incubation either with 25 ng mL^{-1} FGF-2, $250 \mu\text{g mL}^{-1}$ BSA-AGEs alone or BSA-AGEs combined with $10 \mu\text{g mL}^{-1}$ of MCP, MCF or charantin as shown. The bar graph shows the effects of MCP, MCF or charantin on the inhibition of cell proliferation induced by the BSA-AGEs. The data are presented as mean \pm SD ($n = 3$). (B) Representative photomicrographs (40 \times magnification) showing the BAEC measured from the wound edge (indicated by dashed lines) after a 24 hours incubation for the untreated cells (i), or treated either with FGF-2 (ii) or $250 \mu\text{g mL}^{-1}$ BSA-AGEs alone (iii) or combined with $10 \mu\text{g mL}^{-1}$ of MCP (iv), MCF (v) or charantin (vi). The bar graphs (vii) show the number of migrated cells (dark bars) and the distance of migration (clear bars) of the BAEC under these conditions. The data are presented as the mean \pm SD ($n = 3$). (C) Representative photomicrographs (40 \times magnification) showing the BAEC tube formation in cells treated with $250 \mu\text{g mL}^{-1}$ BSA-AGEs alone (i) or combined with $10 \mu\text{g mL}^{-1}$ of MCP (ii), MCF (iii) or charantin (iv) after 24 hours of incubation. The closed areas were counted for quantification of tubulogenesis. The bar graph (v) shows the effects of MCP, MCF extracts and charantin on tube formation. The data are presented as the mean \pm SD ($n = 3$). (*) and (**) indicate statistically significant differences ($p < 0.05$ and $p < 0.01$, respectively) from the control.



centration previously shown to inhibit AGE-induced cell functions following RAGE neutralization,³⁵ and the phosphorylation of ERK1/2 was evaluated in the presence of BSA-AGEs, MCF, MCP extracts or charantin. The isotype control IgG₁ did not affect ERK1/2 phosphorylation induced by 50 $\mu\text{g mL}^{-1}$ BSA-AGEs, compared with the basal expression level of p-ERK1/2 in untreated control cells (Fig. 6A). However, pre-treatment with the neutralizing RAGE antibody prevented the increase in ERK1/2 phosphorylation induced by 50 $\mu\text{g mL}^{-1}$ BSA-AGEs (Fig. 6A). Neutralization of RAGE with the anti-RAGE antibody strongly inhibited the ERK1/2 phosphorylation induced by MC extracts and charantin, while pre-treatment with IgG₁ did not change the increases in p-ERK1/2 levels induced by MC extracts and charantin, compared with the control (Fig. 6A).

Next, the cells were treated with an anti-RAGE antibody or an IgG₁ control, and tubulogenesis was assessed in the presence of BSA-AGEs or MCF. The addition of MC extracts and charantin to IgG₁-pretreated cells surprisingly induced a significant increase in endothelial tube formation (Fig. 6B) as compared with the untreated control cells. However, the addition of either MCF extract (previously shown to have the strongest pro-angiogenic effects) or 10 $\mu\text{g mL}^{-1}$ BSA-AGEs to anti-RAGE antibody-pretreated cells suppressed their pro-angiogenic effects as compared with the untreated control cells (Fig. 6B).

4 Discussion

Momordica charantia is a popular vegetable in Asia for its anti-oxidant, hypoglycemic and therefore anti-diabetic properties, which were recognized more than 600 years ago.^{23,39} Indeed, administration of MC extracts to diabetic rats over 30 days not only reduced hyperglycemia but also reduced lipid peroxidation and increased intracellular production of antioxidants such as superoxide dismutase, catalase and glutathione in heart tissue of diabetic rats.²⁵ Furthermore, MC extracts protected cultured human neuroblastoma cells against intracellular oxidative stress and improved their viability and reduced apoptosis.⁴⁰ As a cheap and potential medicinal plant-based natural therapeutic food, a growing body of evidence supports the beneficial effects of MC extracts on impaired wound-healing in diabetic animal models.^{32,34} However, the molecular mechanisms underlying the pro-angiogenic effects of MC extracts and its ability to protect against AGEs, which are the main cause of diabetic vascular complications including impairment of wound-healing, remained unclear. Here, we have demonstrated that two standardized methanolic extracts of MC (MCP and MCF) and charantin had pro-angiogenic effects *in vitro*. These effects were mediated by interactions with the main receptor for AGEs (RAGE), through which these extracts may reduce the anti-angiogenic effects of a high concentration of AGEs. This study helps improve our understanding of the angiogenic molecular mechanisms underlying use of MC extracts to promote healing in the diabetic wound.

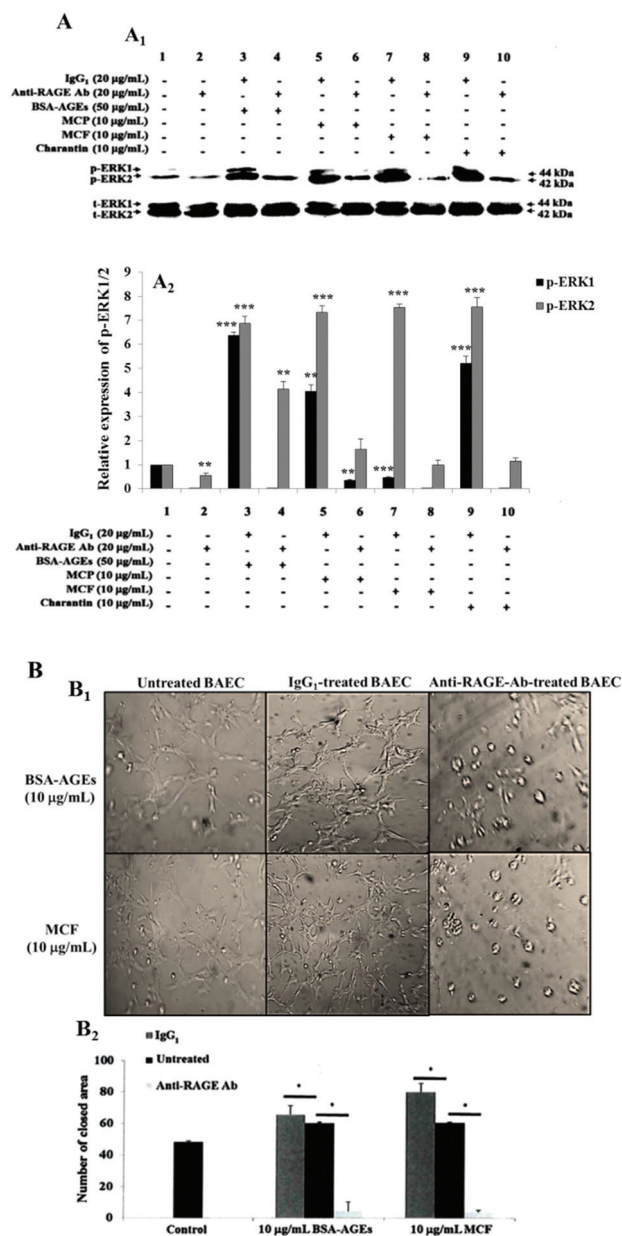


Fig. 6 Effect of RAGE neutralization on the modulation of p-ERK1/2 levels and tube formation by the MC extracts and charantin. (A): (A₁) Representative western blot analysis showing the levels of p-ERK1/2 induced by either 50 $\mu\text{g mL}^{-1}$ BSA-AGEs or 10 $\mu\text{g mL}^{-1}$ MC extracts and charantin in cells treated with the isotype control IgG₁ and anti-RAGE antibody. (A₂) The bar graph shows the densitometric quantification of the bands corresponding to p-ERK1/2 levels expressed as values relative to total-ERK1/2 levels and calculated as the ratio to the levels in the control cultures. The data are presented as the mean \pm SD ($n = 3$). (B₁) Representative photomicrographs (40 \times magnification) showing the BAEC tube formation in untreated cells and pre-treated cells with IgG₁ and anti-RAGE antibody then cultured in the presence or absence of either 250 $\mu\text{g mL}^{-1}$ BSA-AGEs or 10 $\mu\text{g mL}^{-1}$ of MCF for 24 hours of incubation. The closed areas were counted for quantification of tubulogenesis. (B₂) The bar graph shows the loss of MCF-induced tube formation after treatment with a RAGE neutralization antibody, compared with untreated cells (control) and those treated with the isotype control IgG₁. The data are presented as mean \pm SD ($n = 3$). (*), (**) and (***) signify statistically significant differences ($p < 0.05$, $p < 0.01$ and $p < 0.001$, respectively) from the control.



This study used high concentrations of methylglyoxal to prepare BSA-AGEs *in vitro*. This enabled us to produce AGEs in a short time period and reduce the risk of bacterial contamination of protein samples. Such model AGEs have been used previously to study cellular functions.³⁶ To validate our *in vitro* angiogenesis assays, FGF-2 was used as a positive control. This compound is considered as one of the strongest pro-angiogenic growth factor, inducing here a concomitant enhancement of cell proliferation, migration and tube formation. Our results indicate that all of the MC extracts (MCF, MCP and charantin) increased endothelial cell proliferation in a dose-dependent manner. The lowest and the highest concentrations of the MC extracts (*i.e.* 10 and 75 $\mu\text{g mL}^{-1}$) stimulated cell proliferation to a level similar to that induced by FGF-2. However, the intermediate concentration of MC extracts (*i.e.*, 50 $\mu\text{g mL}^{-1}$) stimulated proliferation to a greater level than that induced by FGF-2, indicating the maximal activation of the signaling pathways. This increase of cell proliferation with MC extract concentration in a bell-shaped curve manner suggests a receptor dependent-mechanism, whose optimal stimulation (peak) might correspond to the optimal oligomerization of the receptor.¹⁵ Among the bioactive phytochemical components and proteins previously mentioned, MC extracts contain insulin-like proteins which may stimulate endothelial cell proliferation by acting as an insulin-like growth factor (a pro-angiogenic growth factor) bound to two dimers of insulin receptors followed by the activation of the receptor tyrosine kinase.^{20,41} In addition, a recent study has reported that topical insulin accelerates the skin wound-healing in diabetic rats.⁴² To understand the molecular mechanism involved in the pro-mitogenic effect of charantin it is important to know that charantin is mainly composed of the combination of sterol and glucose metabolites. Glucose is an essential and vital metabolite for cell function and its facilitated transport through the hexose transporter (*e.g.* GLUT1) is accompanied by a linear cell response but cannot explain the bell-shaped curve as previously described, which suggests a receptor-dependent mechanism.^{41,43} Therefore, charantin, which is also considered as a glycosylated phytochemical compound, could be recognized by a receptor for AGEs such as RAGE. Altogether, these findings suggest that MC extracts stimulated endothelial cell proliferation through receptor-dependent mechanisms, which remain to be identified.

In contrast to their similar pro-mitogenic effects on cell proliferation, we showed that the MC extracts and charantin acted differently on the increase in the number of migrated cells using the wound-healing assay. However, MC extracts and charantin enhanced the distance of migration with an efficacy similar to that of FGF-2. MCP extract tested at the highest concentration (*i.e.*, 75 $\mu\text{g mL}^{-1}$) actually inhibited the number of migrated cells, while MCF extract and charantin increased the migrated cell number in a dose-dependent manner with a peak of stimulation at 50 $\mu\text{g mL}^{-1}$, close to the level induced by FGF-2. These methanolic extracts of MCF and MCP contain ascorbigen, a bound form of ascorbic acid, low doses of which have been shown to have pro-angiogenic effects^{20,44} whereas

high doses have anti-angiogenic effects.⁴⁵ An assessment of the content of ascorbigens from each MC extract might explain their differential effects on migrated cell number. Concerning charantin effect, the presence of sterol has been reported to induce changes in the contents of membrane cholesterol and alters the micro-viscosity of the plasma membrane, which in turn can regulate endothelial cell migration.⁴⁶

Regarding tubulogenesis process, which corresponds to the last step of angiogenesis, both MCP and MCF extracts enhanced tube formation in a dose-dependent manner with a peak of stimulation at 50 $\mu\text{g mL}^{-1}$. At this concentration, MCP showed a stimulatory effect similar to that of FGF-2, but the effect of the MCF extract was almost twice that of FGF-2. This finding suggests that MCF extracts might contain more insulin-like proteins or other stimulating agents than the MCP extracts. In contrast to the MCP and MCF extracts, charantin increased tube formation with its increasing concentrations: the stimulatory effect of the lowest concentration was similar to that of FGF-2, but was nearly twice that of FGF-2 effect at the highest concentration. Charantin thus effectively stimulated endothelial tube formation, but its effect was not as great as that induced by the MCF extract. With regards to the charantin effect, the presence of sterol might be involved in the promotion of tubulogenesis through the activation of sterol regulatory element-binding proteins (SREBP), previously demonstrated to play a key role in angiogenesis.⁴⁷ Thus, an assessment of the SREBP activation might reveal the involvement of SREBP in charantin-induced tube formation.

The maximal increase in the p-ERK1/2 expression for the three MC extracts occurred at 50 $\mu\text{g mL}^{-1}$, at the concentration that induced the maximal stimulation of cell proliferation, migration and tube formation. However, FGF-2 had a greater effect on the levels of p-ERK1/2 than the MC extracts, but its effects on the pro-angiogenic responses were similar or smaller. These results suggest that p-ERK1/2 may not be the primary target signaling protein involved in the signal transduction affected by MC extracts and charantin. The expression of a panel of activated phospho-protein expressions should be screened to identify the primary phospho-proteins affected by MC extracts and charantin.

In agreement with previous studies, we showed that methanolic MC extracts and charantin have beneficial effects on AGE-inhibited angiogenesis, which was used as an *in vitro* model mimicking the impaired wound-healing in diabetic patients. Here, we confirmed that a high dose of BSA-AGEs (250 $\mu\text{g mL}^{-1}$) inhibit angiogenesis, as reported previously.⁴⁸ These authors showed that 500 $\mu\text{g mL}^{-1}$ BSA-AGEs inhibit retinal vascular cell proliferation, whereas at low doses of BSA-AGEs (62.5–100 $\mu\text{g mL}^{-1}$) induce these angiogenic processes.^{13,48} In addition, high concentrations of BSA-AGEs have been reported to impair cell migration, adhesion and secretion of vasoactive substances by late bone marrow-derived endothelial progenitor cells, which are important in neovascularization.²⁹ Therefore, in diabetic patients, the local accumulation of AGEs in the vessel wall or within the tissue may impair the neovascularization process by interfering with the cell-matrix



interactions. The biological effects of AGEs are mainly mediated through interactions with the AGE-specific receptor, RAGE. RAGE is a multi-ligand signal transduction receptor and its protein expression is induced by AGEs and is over-expressed in diabetic conditions.⁴⁹ Shoji and colleagues⁵⁰ performed an *in vivo* study that compared the responses of non-diabetic mice to those of RAGE^{−/−} mice. The study demonstrated that adenovirus-mediated over-expression of endogenous secreted RAGE, a decoy receptor for RAGE, corrects the diabetes-associated impairment of angiogenic responses *in vivo*. These findings support the suggestion that RAGE is involved in impairment of angiogenesis as seen in diabetic wound-healing whereas blockade of RAGE receptors may have a potential therapeutic effect. This study also demonstrated that the neutralization of the RAGE receptor utilizing a specific monoclonal antibody suppressed the phosphorylation of ERK1/2, the activation of the key angiogenic signaling protein, induced by all of the MC extracts including charantin and inhibited the tube formation induced by MCF extract (selected for its strongest tubulogenic effect). These important findings highlighted the presence of biologically active proteins and phytochemicals in MC extracts mediating RAGE activation, which remain to be clarified. Furthermore, the MC extracts could act not only by binding to RAGE but also by binding to the BSA-AGEs thus preventing their interaction with RAGE.

Here we also observed that MC extracts combined with high AGE concentration not only reduced anti-angiogenic effects of AGEs but also reversed tubulogenesis process. Beyond their pro-angiogenic effects, MC extracts have been recently identified from a clinical study in diabetic patients as potent natural compounds for the prevention of AGE formation, which was demonstrated to restore angiogenesis.³⁹ An *in vivo* study demonstrated that aqueous extracts of MC improve wound-healing in albinos rats; this beneficial effect was linked to increased production of extracellular matrix proteins and hydroxyproline, a constituent of collagen that plays a key role in collagen stability.³¹ Importantly, increased production of collagen facilitates endothelial tube formation. This finding is consistent with the increased tube formation induced by the MC extracts even when added to high concentration of BSA-AGEs. In addition to laminin, the type I collagen fibrils are a major component of MatrigelTM, and this material has been reported to promote rapid vascular tube formation.⁵¹ The hypothesis that the MC extracts caused an increase in protein synthesis in the BAEC remains to be investigated. The discrepancies between endothelial cell proliferation/migration and tube formation suggest that the MC extracts counteracted the anti-angiogenic effects of the AGEs by distinct mechanisms, one of which may be receptor-dependent through binding competitiveness between MC extracts and AGEs high concentration to RAGE receptor.

In conclusion, our results of this *in vitro* study show that MC extracts and charantin exert strong pro-angiogenic effects. These observations support the beneficial effects of topical MC extracts on wound-healing. Although the MC extracts and charantin contain different biologically active constituents, we

found that RAGE was involved in the stimulation of angiogenesis, including cell signaling and tubulogenesis, by these extracts. Thus, further study of the structure–function relationships of the MC extracts might facilitate the development of new therapies to promote wound-healing using natural pro-angiogenic compounds.

Abbreviations

AGEs	Advanced glycation endproducts
BAEC	Bovine aortic endothelial cells
BSA	Bovine serum albumin
DMEM	Dulbecco's modified Eagle medium
EDTA	Ethylene-diamine-tetra-acetic acid
FBS	Fetal bovine serum
FGF-2	Fibroblast growth factor-2
MC	<i>Momordica charantia</i>
MCF	<i>Momordica charantia</i> flesh
MCP	<i>Momordica charantia</i> pulp
PBS	Phosphate buffered saline
SDS-PAGE	Sodium dodecyl sulfate-polyacrylamide gel electrophoresis
p-ERK	Phosphorylated extracellular signal-regulated kinase
SPM	Serum-poor medium
RAGE	Receptor for advanced glycation endproducts

Conflicts of interest

There are no conflicts of interest to declare.

Acknowledgements

We would like to thank the Prince Sultan Medical Military City and the Saudi Ministry of Higher Education for providing a PhD scholarship to Ali Aljohi allowing him to undertake this study.

References

- 1 S. A. Tabish, Is diabetes becoming the biggest epidemic of the twenty-first century?, *Int. J. Health Sci.*, 2007, **1**, V–VIII.
- 2 T. Synold, B. Xi, G. E. Wuenschell, D. Tamae, J. L. Figarola, S. Rahbar and J. Termini, Advanced glycation endproducts of DNA: quantification of N²-(1-carboxyethyl)-2'-deoxyguanosine (CEdG) in biological samples by LC-ESI-MS/MS, *Chem. Res. Toxicol.*, 2008, **21**, 2148–2155.
- 3 M. Bohlooli, A. A. Moosavi-Movahedi, F. Taghavi, A. A. Sabovry, P. Maghami, A. Seyedarabi, F. Moosavi-Movahedi, F. Ahmad, A. Shockravi and M. Habibi-Rezaei, Inhibition of fluorescent advanced glycation endproducts (AGEs) of human serum albumin upon incubation



- with 3 β -hydroxybutyrate, *Mol. Biol. Rep.*, 2014, **41**, 3705–3713.
- 4 A. Goldin, J. A. Beckman, A. M. Schmidt and M. A. Creager, Advanced glycation endproducts: sparking the development of diabetic vascular injury, *Circulation*, 2006, **114**, 597–605.
 - 5 M. Pia de la Maza, F. Garrido, N. Escalante, L. Leiva, G. Barrera, S. Schnitzler, M. Zanolli, J. Verdaguer, S. Hirsch, N. Jara and D. Bunout, Fluorescent advanced glycation endproducts (AGEs) detected by spectro-photo-fluorimetry, as a screening tool to detect diabetic microvascular complications, *J. Diabetes Mellitus*, 2012, **2**, 221–226.
 - 6 D. Pepe, C. G. Elliott, T. L. Forbes and D. W. Hamilton, Detection of galectin-3 and localization of advanced glycation endproducts (AGE) in human chronic skin wounds, *Histol. Histopathol.*, 2014, **29**, 251–258.
 - 7 C. H. Park, T. Tanaka, H. Y. Kim, J. C. Park and T. Yokozawa, Protective effects of corni fructus against advanced glycation endproducts and radical scavenging, *Evid. Based Complement. Alternat. Med.*, 2012, **2012**, 418953.
 - 8 B. S. Bradke and D. Vashishth, N-phenacylthiazolium bromide reduces bone fragility induced by nonenzymatic glycation, *PLoS One*, 2014, **9**, e103199.
 - 9 A. Stirban, T. Gawlowski and M. Roden, Vascular effects of advanced glycation endproducts: clinical effects and molecular mechanisms, *Mol. Metab.*, 2014, **3**, 94–108.
 - 10 V. P. Singh, A. Bali, N. Singh and A. S. Jaggy, Advanced glycation endproducts and diabetic complications, *Korean J. Physiol. Pharmacol.*, 2014, **18**, 1–14.
 - 11 N. Singh, D. G. Armstrong and B. A. Lipsky, Preventing foot ulcers in patients with diabetes, *J. Am. Med. Assoc.*, 2005, **293**, 217–228.
 - 12 M. S. Huijberts, N. C. Schaper and C. G. Schalkwijk, Advanced glycation endproducts and diabetic foot disease, *Diabetes Metab. Res. Rev.*, 2008, **24**, S19–S24.
 - 13 T. Okamoto, S. Tanaka, A. C. Stan, T. Koike, M. Kase, Z. Makita, H. Sawa and K. Nagashima, Advanced glycation endproducts induce angiogenesis *in vivo*, *Microvasc. Res.*, 2002, **63**, 186–195.
 - 14 A. W. Stitt, C. McGoldrick, A. Rice-McCaldin, D. R. McCance, J. V. Glenn, D. K. Hsu, F. T. Liu, S. R. Thorpe and T. A. Gardiner, Impaired retinal angiogenesis in diabetes: role of advanced glycation endproducts and galectin-3, *Diabetes*, 2005, **54**, 785–794.
 - 15 R. G. Posner, J. Bold, Y. Bernstein, J. Rasor, J. Braslow, W. S. Hlavacek and A. S. Perelson, Measurement of receptor crosslinking at the cell surface via multiparameter flow cytometry, *Proc. SPIE 3256 Advances in Optical Biophysics*, 1998, **3256**, 132–143.
 - 16 K. Tanaka, M. Abe and Y. Sato, Roles of extracellular signal-regulated kinase 1/2 and p38 mitogen-activated protein kinase in the signal transduction of basic fibroblast growth factor in endothelial cells during angiogenesis, *Jpn. J. Cancer Res.*, 1999, **90**, 647–654.
 - 17 E. Boras, B. Gilmore, J. Krupinski, L. A. Potempa, M. Slevin and S. Matou-Nasri, Common angiogenic signalling pathways induced by monomeric C-reactive protein and FGF-2 through MAPK and PI3K, *Eur. J. Exp. Biol.*, 2017, **7**, 18.
 - 18 Y. Yamamoto and H. Yamamoto, RAGE-mediated inflammation, type 2 diabetes, and diabetic vascular complications, *Front. Endocrinol.*, 2013, **4**, 105.
 - 19 S. R. Kumar, J. Ashish and N. Satish, *Momordica charantia* Linn: A mini review, *Int. J. Biomed. Res.*, 2011, **2**, 579–587.
 - 20 D. S. Kumar, K. V. Sharathnath, P. Yogeswaran, A. Harani, K. Sudhakar, P. Sudha and D. Banji, A medicinal potency of *Momordica charantia*, *Int. J. Pharm. Sci. Rev. Res.*, 2010, **1**, Article 018.
 - 21 J. Singh, E. Cumming, G. Manoharan, H. Kalasz and E. Adehate, Medicinal chemistry of the anti-diabetic effects of *Momordica charantia*: active constituents and modes of actions, *Open Med. Chem. J.*, 2011, **5**, 70–77.
 - 22 J. Virdi, S. Sivakami, S. Shahani, A. C. Suthar, M. M. Banavalikar and M. K. Biyani, Antihyperglycemic effects of three extracts from *Momordica charantia*, *J. Ethnopharmacol.*, 2003, **88**, 107–111.
 - 23 L. Leung, R. Birtwhistle, J. Kotecha, S. Hannah and S. Cuthbertson, Anti-diabetic and hypoglycaemic effects of *Momordica charantia* (bitter melon): a mini review, *Br. J. Nutr.*, 2009, **102**, 1703–1708.
 - 24 P. Chaturvedi, Antidiabetic potentials of *Momordica charantia*: multiple mechanisms behind the effects, *J. Med. Food*, 2012, **15**, 101–107.
 - 25 U. N. Tripathi and D. Chandra, The plant extracts of *Momordica charantia* and *Trigonella foenum-graecum* have anti-oxidant and anti-hyperglycemic properties for cardiac tissue during diabetes mellitus, *Oxid. Med. Cell. Longevity*, 2009, **2**, 290–296.
 - 26 M. Z. Nasseem, S. R. Patil and S. B. Ravindra Patil, Antispermato-genic and androgenic activities of *Momordica charantia*, (Karela) in albino rats, *J. Ethnopharmacol.*, 1998, **61**, 9–16.
 - 27 H. D. Coutinho, J. G. Costa, V. S. Falcão-Silva, J. P. Siqueira-Júnior and E. O. Lima, Effect of *Momordica charantia* L. in the resistance to aminoglycosides in methicillin-resistant *Staphylococcus aureus*, *Comp. Immunol. Microbiol. Infect. Dis.*, 2010, **33**, 467–471.
 - 28 H. L. Cheng, C. Y. Kuo, Y. W. Liao and C. C. Lin, EMCD, a hypoglycemic triterpene isolated from *Momordica charantia* wild variant, attenuates TNF- α -induced inflammation in FL83B cells in an AMP-activated protein kinase-independent manner, *Eur. J. Pharmacol.*, 2012, **689**, 241–248.
 - 29 C. J. Li, S. F. Tsang, C. H. Tsai, H. Y. Tsai, J. H. Chyuan and H. Y. Hsu, *Momordica charantia* extract induces apoptosis in human cancer cells through caspase- and mitochondria-dependent pathways, *Evid. Based Complement. Alternat. Med.*, 2012, **2012**, 261971.
 - 30 S. Alam, M. Asad, S. M. Asdaq and V. S. Prasad, Antiulcer activity of methanolic extract of *Momordica charantia* L. in rats, *J. Ethnopharmacol.*, 2009, **123**, 464–469.



- 31 R. Prashanthi, N. Mohan and G. V. Siva, Wound healing property of aqueous extract of seed and outer layer of *Momordica charantia* L. on albino rats, *Indian J. Sci. Technol.*, 2012, **5**, 1936–1940.
- 32 S. L. Teoh, A. A. Latiff and S. Das, The effect of topical extract of *Momordica charantia* (bitter gourd) on wound healing in nondiabetic rats and in rats with diabetes induced by streptozotocin, *Clin. Exp. Dermatol.*, 2009, **34**, 815–822.
- 33 S. Sharma, M. C. Sharma, D. V. Kohli and S. C. Chaturvedi, Formulation, evaluation, wound healing studies of benzene-95% absolute ethanol extract of leaves, *J. Optoelectronics Biomed. Mat.*, 2009, **1**, 375–378.
- 34 A. Pişkin, B. Z. Altunkaynak, G. Tümentemur, S. Kaplan, O. B. Yazici and M. Hökelek, The beneficial effects of *Momordica charantia* (bitter gourd) on wound healing of rabbit skin, *J. Dermatol. Treat.*, 2014, **25**, 350–357.
- 35 R. Singh, I. Garcia-Gomez, K. Gudehithlu and A. K. Singh, Bitter melon extract promotes granulation tissue growth and angiogenesis in the diabetic wound, *Adv. Skin Wound Care*, 2017, **30**, 16–26.
- 36 H. Sharaf, S. Matou-Nasri, Q. Wang, Z. Rabhan, H. Al-Eidi, A. Al Abdulrahman and N. Ahmed, Advanced glycation end-products increase proliferation, migration and invasion of the breast cancer cell line MDA-MB-231, *Biochim. Biophys. Acta*, 2015, **1852**, 429–441.
- 37 A. Sattar, P. Rooney, S. Kumar, D. Pye, D. C. West, I. Scott and P. Ledger, Application of angiogenic oligosaccharides of hyaluronan increases blood vessel numbers in rat skin, *J. Invest. Dermatol.*, 1994, **103**, 576–579.
- 38 J. Angulo and S. Matou, Application of mathematical morphology to the quantification of *in vitro* endothelial cell organization into tubular-like structures, *Cell Mol. Biol.*, 2007, **53**, 22–35.
- 39 W. Trakoon-Osot, U. Sotanaphum, P. Phanachet, S. Porasuphatana, U. Udomsubpayakul and S. Komindr, Pilot study: Hypoglycemic and antiglycation activities of bitter melon (*Momordica charantia* L.) in type 2 diabetic patients, *J. Pharm. Res.*, 2013, **6**, 859–864.
- 40 K. B. Kim, S. A. Lee, I. Kang and J.-H. Kim, *Momordica charantia* ethanol extract attenuates H₂O₂-induced cell death by its antioxidant and anti-apoptotic properties in human neuroblastoma SK-N-MC cells, *Nutrients*, 2018, **10**, 1368.
- 41 H. K. Bid, J. Zhan, D. A. Phelps, R. T. Kurmasheva and P. J. Houghton, Potent inhibition of angiogenesis by the IGF-1 receptor-targeting antibody SCH717454 is reversed by IGF-2, *Mol. Cancer Ther.*, 2012, **11**, 649–659.
- 42 M. H. Lima, A. M. Caricilli, L. L. de Abreu, E. P. Araujo, F. F. Pelegrinelli, A. C. Thirone, D. M. Tsukumo, A. F. Pessoa, M. F. dos Santos, M. A. de Moraes, J. B. Carvalheira, L. A. Velloso and M. J. Saad, Topical insulin accelerates wound healing in diabetes by enhancing the AKT and ERK pathways: a double-blind placebo-controlled clinical trial, *PLoS One*, 2012, **7**, e36974.
- 43 C. D. Young, A. S. Lewis, M. C. Rudolph, M. D. Ruehle, M. R. Jackman, U. J. Yun, O. Ilkun, R. Pereira, E. D. Abel and S. M. Anderson, Modulation of glucose transporter 1 (GLUT1) expression levels alters mouse mammary tumor cell growth *in vitro* and *in vivo*, *PLoS One*, 2011, **6**, e23205.
- 44 S. Telang, A. L. Clem, J. W. Eaton and J. Chesney, Depletion of ascorbic acid restricts angiogenesis and retards tumor growth in a mouse model, *Neoplasia*, 2007, **9**, 47–56.
- 45 N. A. Mikirova, T. E. Ichim and N. H. Riordan, Anti-angiogenic effect of high doses of ascorbic acid, *J. Transl. Med.*, 2008, **6**, 50.
- 46 Z. Hong, M. C. Staiculescu, P. Hampel, I. Levitan and G. Forgacs, How cholesterol regulates endothelial biomechanics, *Front. Physiol.*, 2012, **3**, 426.
- 47 M. Yao, R. H. Zhou, M. Petreaca, L. Zheng, J. Shyy and M. Martins-Green, Activation of sterol regulatory element-binding proteins (SREBPs) is critical in IL-8-induced angiogenesis, *J. Leukocyte Biol.*, 2006, **80**, 608–620.
- 48 R. Chibber, P. A. Molinatti, N. Rosatto, B. Lambourne and E. M. Kohner, Toxic action of advanced glycation endproducts on cultured retinal capillary pericytes and endothelial cells: relevance to diabetic retinopathy, *Diabetologia*, 1997, **40**, 156–164.
- 49 S. Matou-Nasri, H. Sharaf, Q. Wang, N. Almobadel, Z. Rabhan, H. Al-Eidi, W. B. Yahya, T. Trivilegio, R. Ali, N. Al-Shanti and N. Ahmed, Biological impact of advanced glycation endproducts on estrogen receptor-positive MCF-7 breast cancer cells, *Biochim. Biophys. Acta*, 2017, **1863**, 2808–2820.
- 50 T. Shoji, H. Koyama, T. Morioka, S. Tanaka, A. Kizu, K. Motoyama, K. Mori, S. Fukumoto, A. Shioi, N. Shimogaito, M. Takeuchi, Y. Yamamoto, H. Yonekura, H. Yamamoto and Y. Nishizawa, Receptor for advanced glycation endproducts is involved in impaired angiogenic response in diabetes, *Diabetes*, 2006, **55**, 2245–2255.
- 51 C. J. Jackson and K. L. Jenkins, Type I collagen fibrils promote rapid vascular tube formation upon contact with the apical side of cultured endothelium, *Exp. Cell Res.*, 1991, **192**, 319–323.

